Single-frequency laser spectroscopy of the boron bound exciton in ^{28}Si

A. Yang,[1] M. Steger,[1] T. Sekiguchi,[1] D. Karaiskaj,[1] M. L. W. Thewalt,[1] M. Cardona,[2] K. M. Itoh,[3] H. Riemann,[4] N. V. Abrosimov,[4] M. F. Churbanov,[5] A. V. Gusev,[5] A. D. Bulanov,[5] I. D. Kovalev,[5] A. K. Kaliteevskii,[6] O. N. Godisov,[6] P. Becker,[7] H.-J. Pohl,[8] J. W. Ager III,[9] and E. E. Haller[9]

[1]*Department of Physics, Simon Fraser University, Burnaby, British Columbia, Canada V5A 1S6*
[2]*Max-Planck-Institut für Festkörperforschung, 70569 Stuttgart, Germany*
[3]*Keio University and CREST–JST, Yokohama 223-8522, Japan*
[4]*Institute for Crystal Growth (IKZ), 12489 Berlin, Germany*
[5]*IChHPS, RAS, 603000 Nizhny Novgorod, Russia*
[6]*Science and Technical Center "Centrotech," 198096 St. Petersburg, Russia*
[7]*Physikalisch-Teknische Bundestanstalt Braunschweig, 38116 Braunschweig, Germany*
[8]*VITCON Projectconsult GmbH, 07743 Jena, Germany*
[9]*University of California–Berkeley and LBNL, Berkeley, California 94720, USA*

(Received 18 August 2009; revised manuscript received 11 September 2009; published 11 November 2009)

While the first comparison of shallow bound exciton photoluminescence between natural Si and highly enriched ^{28}Si dramatically demonstrated the importance of inhomogeneous isotope broadening, the transitions in ^{28}Si were in fact too narrow to be resolved with the then available instrumental resolution of 0.014 cm^{-1}. We report results for the boron bound exciton transition in highly enriched ^{28}Si using a novel apparatus for photoluminescence excitation spectroscopy based on a tuneable single-frequency laser source with sub-MHz resolution. Twenty well-resolved doublets, exhibiting a $^{10}B-^{11}B$ isotope splitting, are observed in the new spectra for ^{28}Si with isotopic enrichment >99.99%. Linewidths as narrow as 0.0012 cm^{-1} (150 neV) full width at half maximum are observed for the most highly enriched sample.

DOI: 10.1103/PhysRevB.80.195203 PACS number(s): 78.55.Ap, 71.35.−y, 71.55.Cn

I. INTRODUCTION

The effects of isotopic composition on the properties of semiconductors has been the subject of numerous recent studies, as detailed in several reviews.[1–5] Despite the technological importance of Si and its central role in the development of semiconductor physics and spectroscopy, studies of isotope effects on indirect band-gap transitions in Si had long been delayed due to the lack of suitable samples. In the first such study, Karaiskaj *et al.*[6] used photoluminescence (PL) spectroscopy to observe significantly sharper bound-exciton (BE) transitions in the no-phonon region in highly enriched (99.896%) ^{28}Si as compared to natural Si (^{nat}Si), even though the ^{28}Si sample was of only moderate chemical purity ($[B]\sim 7\times 10^{14}$ cm^{-3} and $[P]\sim 7\times 10^{13}$ cm^{-3}). In ^{nat}Si, the no-phonon P BE transition has a linewidth of 0.041 cm^{-1} full width at half maximum (FWHM), whereas the observed linewidth of the same transition in the ^{28}Si sample was 0.014 cm^{-1}, essentially identical to the maximum available instrumental resolution of the Fourier-transform spectrometer used in the study. The apparent inhomogeneous isotope broadening inherent in ^{nat}Si was attributed to local fluctuations in the band-gap energy resulting from statistical fluctuations in the isotopic composition within the (~3.5 nm) effective radius of the bound exciton. This effect is not accounted for within the virtual-crystal approximation, which treats every atom in the crystal as having the same mass—the average atomic mass. In the same study, it was found that there exists a 0.92 cm^{-1} decrease in the indirect band-gap energy of highly enriched ^{28}Si relative to ^{nat}Si, which was explained as being due mainly to the electron-phonon renormalization. Shifts of the wave-vector-conserving phonon energies were also observed.

A similar reduction in the no-phonon linewidths in ^{28}Si was seen for the components of the B BE line, which had been found to have nine resolved components in ^{nat}Si.[7] The existence of nine distinct components was explained as resulting from a threefold splitting of the electron levels of the BE due to the valley-orbit interaction, coupled with a threefold splitting of the hole states due to hole-hole coupling. More detailed studies of the B BE followed, involving uniaxial stress[8] and Zeeman[9] perturbations, and revealed that a complete description required the inclusion of additional effects, such as the coupling of the hole angular momentum with the electron spin. Much like what was seen for the P BE, the linewidths of the components of the B BE were found to be much narrower in ^{28}Si than in ^{nat}Si, with the narrowest components having an observed FWHM of 0.017 cm^{-1}, slightly larger than that of the P BE. As a result of the increased spectral resolution, 14 components were resolved in the B BE spectrum in ^{28}Si. This new fine structure was well accounted for by the earlier investigations of the effects of uniaxial stress and magnetic fields on the B BE.[8,9]

The inability to fully resolve the no-phonon BE transitions in the ^{28}Si PL spectrum demonstrated the limitations of the Fourier transform spectrometer, which led to the development of a novel apparatus for photoluminescence excitation (PLE) spectroscopy based on a tuneable single-frequency laser source with sub-MHz resolution, allowing for a major increase in instrumental resolution. Using this new apparatus, linewidths as narrow as 0.0019 cm^{-1} FWHM have been observed[10] for the no-phonon B BE transition in a ^{28}Si sample with isotopic enrichment of 99.991%. In the present study, we use PLE spectroscopy to reveal previously unseen fine structure in the B BE spectrum and investigate

 ©2009 The American Physical Society

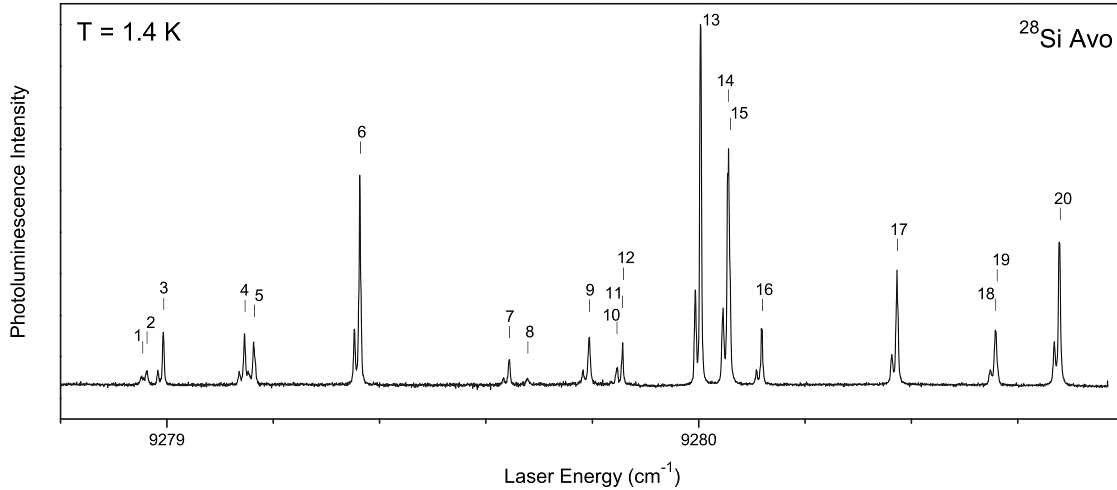

FIG. 1. Photoluminescence excitation spectrum of the no-phonon boron bound exciton transitions for a sample of ^{28}Si with isotopic enrichment of 99.995%. Twenty transitions are observed in this spectrum with each transition consisting of a doublet with an intensity ratio reflecting the 80/20 natural abundance ratio of ^{11}B/^{10}B. The stronger ^{11}B components are labeled 1–20 in order of increasing energy.

effects due to Si isotopic composition, sample temperature, and the application of an external magnetic field.

II. EXPERIMENT

In order to overcome the resolution limit imposed by commercial spectrometers and the weak luminescence signals characteristic of bound excitons in Si, the no-phonon transitions of the BE are studied in absorption rather than in emission, using a single-frequency laser source with a linewidth of less than 70 kHz ($\sim 3\times 10^{-6}$ cm^{-1}) (more than adequate to resolve BE linewidths at their fundamental limit–shallow BE lifetimes in Si are in the 100 ns–1 μs range[11]). The weak absorption and resulting luminescence signal are detected using the transverse optical (TO) wave-vector-conserving phonon replica, which is well separated in energy from the no-phonon transition ($\sim$470 cm^{-1} lower in energy).

An improved sample of ^{28}Si with isotopic enrichment of 99.995% (^{28}Si Avo) was used for the present study. Three other samples, enriched to 99.991% (^{28}Si a), 99.983% (^{28}Si b), and 99.92% (^{28}Si c), were used for comparing the B BE linewidths of samples having different isotopic enrichment.

The basic PLE apparatus used in this study consists of a distributed feedback Yb-doped fiber laser that is fed into a Yb-doped fiber amplifier and is locked and scanned with respect to a stabilized reference cavity, providing a long-term frequency stability of one part in 10^8, and sub-MHz frequency resolution. The beam is mechanically chopped to allow for lock-in detection of the signal and focused onto the edge of the sample, which is loosely mounted (to avoid strain) in a reflecting cavity to optimize the weak luminescence signals, and immersed in superfluid He at a temperature of 1.4 K. A $\frac{3}{4}m$ double monochromator is used to separate the TO phonon-assisted luminescence signal from the scattered excitation radiation. The spectral resolution of $\sim$2 meV ($\sim$16 cm^{-1}) is sufficient to reject both the scattered laser excitation as well as the zone-center optical-phonon Raman scattering but is much wider than the boron BE spectrum so the detection is not selective. The signal is then detected using a liquid-nitrogen-cooled Ge PIN photodiode.

III. RESULTS AND DISCUSSION

The PLE spectrum of the no-phonon B BE transitions for the ^{28}Si sample with isotopic enrichment of 99.995% (^{28}Si Avo) is shown in Fig. 1. Twenty ground-state transitions are observed with the narrowest line having a FWHM of 0.0012 cm^{-1} ($\frac{E}{\Delta E}=8\times 10^6$). Each transition consists of a doublet with a splitting of $\sim$0.01 cm^{-1} and an identical $\sim$80/20 intensity ratio. This doublet arises from the difference in binding energy of excitons localized on ^{10}B and ^{11}B neutral acceptors with the intensity ratio reflecting the $\sim$80/20 natural abundance ratio of ^{11}B/^{10}B. The stronger component at higher energy in each doublet is due to ^{11}B. While isotope splittings have previously been observed[12] for much deeper BE in other semiconductors, no such observations have been reported for a BE transition as shallow as that of the boron BE in silicon. The difference in bound-exciton binding energy observed in this spectrum agrees well with the prediction from the Haynes rule[13] for silicon, based on the $\sim$0.15 cm^{-1} difference in acceptor ionization energy between ^{11}B and ^{10}B previously observed[14–16] in ^{28}Si using midinfrared absorption spectroscopy.

The energy, integrated intensity, and FWHM, of the stronger ^{11}B component for each of the 20 transitions are listed in Table I, along with the boron-isotope splitting for each corresponding doublet. For the majority of the lines, the observed boron-isotope splitting is close to 0.010 cm^{-1}; however, in three cases the splitting is noticeably larger. Line 7 has a boron-isotope splitting of 0.0111(2) cm^{-1} while Line 9 and Line 15 have even larger splittings of 0.0118(2) cm^{-1} and 0.0119(3) cm^{-1}, respectively. This likely results from differences in the B BE wave functions which lead to different electronic-charge densities on the B impurity for the different BE states since it is this difference in charge density

TABLE I. Energy, integrated intensity, FWHM, boron-isotope splitting, and inhomogeneous splitting for each of the 20 boron bound exciton transitions in the ^{28}Si Avo sample as shown in Fig. 1. The values are given for the stronger ^{11}B component in each of the transitions.

Line	Energy (cm^{-1})	Integrated intensity	FWHM (cm^{-1})	Boron-isotope splitting (cm^{-1})	Inhomogeneous splitting (cm^{-1})
1	9278.9545(2)	0.02	0.0019(4)	0.0100(5)	0.0008(2)
2	9278.9626(1)	0.05	0.0021(2)	0.0100(4)	0.0008(2)
3	9278.9939(1)	0.14	0.0019(2)	0.0101(2)	0.0008(1)
4	9279.1470(1)	0.14	0.0015(1)	0.0100(2)	0
5	9279.1646(1)	0.15	0.0023(1)	0.0101(2)	0
6	9279.3639(1)	0.63	0.0019(1)	0.0103(2)	0.0006(1)
7	9279.6443(1)	0.08	0.0015(1)	0.0111(2)	0
8	9279.6787(1)	0.02	0.0017(2)	0.0104(4)	0
9	9279.7949(1)	0.18	0.0033(1)	0.0118(2)	0
10	9279.8462(3)	0.03	0.002 (1)	0.010 (1)	0.0008(3)
11	9279.8568(1)	0.05	0.0013(1)	0.010 (1)	0
12	9279.8582(1)	0.05	0.0013(1)	0.0100(3)	0
13	9280.0044(1)	1	0.0012(1)	0.0099(2)	0
14	9280.0560(1)	0.59	0.0018(1)	0.0100(2)	0
15	9280.0594(1)	0.35	0.0026(2)	0.0119(3)	0
16	9280.1201(1)	0.17	0.0021(2)	0.0098(3)	0.0007(1)
17	9280.3738(1)	0.37	0.0024(1)	0.0099(2)	0.0008(1)
18	9280.5585(1)	0.13	0.0016(2)	0.0098(3)	0
19	9280.5611(1)	0.10	0.0020(2)	0.0098(4)	0
20	9280.6797(1)	0.52	0.0025(1)	0.0097(2)	0

between the initial and final states that produces the isotope shift, via small changes in the energy of the zero-point local vibrational-mode energy of the center.[12] Fig. 2 shows a particular case where two nearby transitions have different boron-isotope splittings. Line 14 exhibits a boron isotope splitting of 0.0100(2) cm^{-1} while for Line 15 this splitting is 0.0119(3) cm^{-1}, resulting in a greater overlap of the two ^{10}B components as compared to the ^{11}B components. The calculation of such effects would require accurate electron and hole wave functions for the different BE states, which are not available.

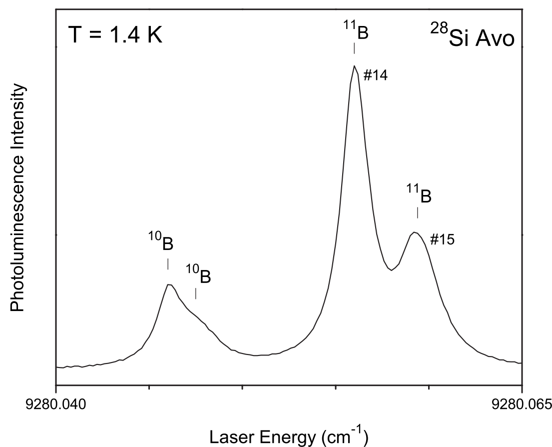

FIG. 2. Photoluminescence excitation spectrum of Lines 14 and 15, revealing a difference in the boron-isotope splitting for two nearby transitions. Line 14 has a boron isotope splitting of 0.0100(2) cm^{-1} while Line 15 has a larger splitting of 0.0119(3) cm^{-1}.

Several of the transitions in the B BE spectrum for the "^{28}Si Avo" sample in Fig. 1 exhibit a small (<0.001 cm^{-1}) splitting of the individual ^{10}B and ^{11}B components. This splitting was found to increase correspondingly for samples of lower silicon-isotopic enrichment and can therefore be attributed to the remaining isotopic randomness in the ^{28}Si samples. This inhomogeneous splitting, similar to an acceptor ground-state splitting which had previously been observed[17] for the Al, Ga, and In BE transitions in comparisons between ^{nat}Si and ^{28}Si, should vanish in samples of higher isotopic enrichment than those available for the present study.

An inhomogeneous splitting is observed for seven of the twenty transitions in the B BE spectrum with the measured values for the ^{28}Si Avo sample listed in Table I. A comparison of Line 6, which exhibits an inhomogeneous splitting, with Line 13, which is not split by the isotopic randomness, is shown in Fig. 3 for the four ^{28}Si samples of different isotopic enrichment. The splitting (denoted by Δ) of Line 6 and the FWHM of Line 13 for the four samples are listed in Table II and are both seen to scale in a similar fashion with isotopic enrichment (ε). Both scale within a factor of two, with $\sqrt{1-\varepsilon}$, which is used as a measure of the inhomogeneous isotope broadening for the present case of $\varepsilon \approx 1$.

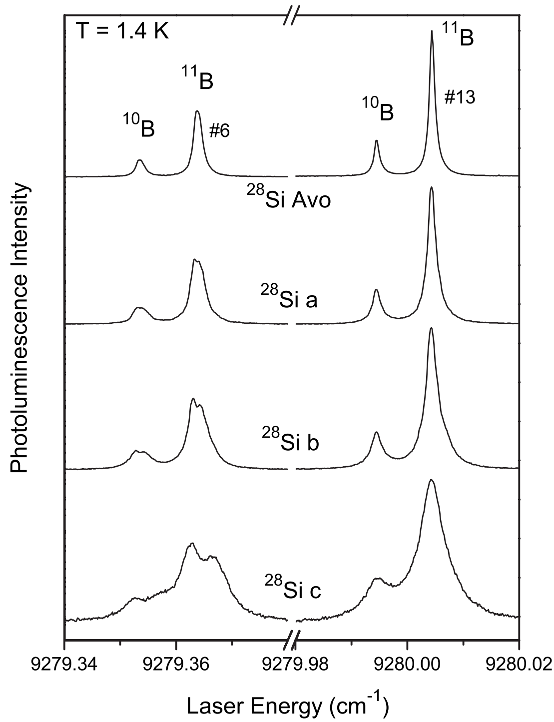

FIG. 3. Photoluminescence excitation spectrum of Lines 6 and 13, for the four ^{28}Si samples. The remaining isotopic inhomogeneity, which increases from top to bottom, is seen to produce only a broadening for Line 13, but both a broadening and a splitting for Line 6.

The linewidths of the transitions in the B BE spectrum are also seen to vary with temperature. A comparison of the width of Line 7 at various liquid He bath temperatures (measured by monitoring the He vapor pressure) between 1.4 and 4.2 K, for the "^{28}Si a" sample, reveals a broadening of the line with increasing temperature, as shown in the plot of FWHM versus temperature in Fig. 4. Assuming that the FWHM of this transition consists of a temperature-independent component and a temperature-dependent component that is proportional to a Bose-Einstein factor, the data in Fig. 4 can be fit to an expression with the functional form

$$\mathrm{FWHM} = \sqrt{A^2 + \left(\frac{B}{e^{C/k_BT} - 1}\right)^2}, \tag{1}$$

TABLE II. Comparison of the inhomogeneous splitting (denoted by Δ) of Line 6 and the FWHM of Line 13, for ^{28}Si samples of different isotopic enrichment (ε). The ratios of Δ, FWHM, and $\sqrt{1-\varepsilon}$ with respect to the values for the ^{28}Si Avo sample are listed in brackets.

Sample	ε	Δ (cm^{-1})	FWHM (cm^{-1})	$\sqrt{1-\varepsilon}$
^{28}Si Avo	0.99995	0.0006 [1]	0.0012 [1]	0.00707 [1]
^{28}Si a	0.99991	0.0012[2.0]	0.0020[1.7]	0.00949[1.3]
^{28}Si b	0.99983	0.0014[2.3]	0.0029[2.4]	0.0130[1.8]
^{28}Si c	0.9992	0.0048[8.0]	0.0064[5.3]	0.028[4.0]

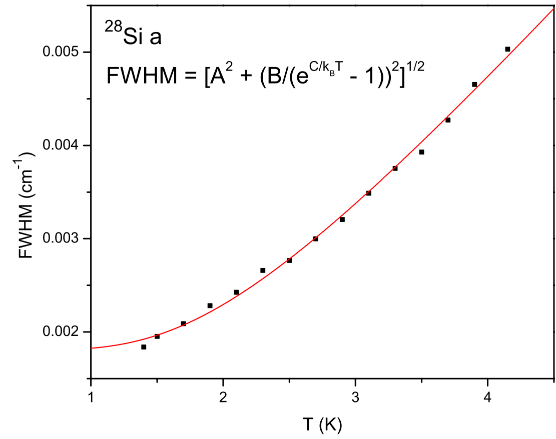

FIG. 4. (Color online) Plot of the FWHM of Line 7 versus He bath temperature for the ^{28}Si a sample. A curve fit to the data (shown by the solid curve) using the expression: FWHM $=\sqrt{A^2+(\frac{B}{e^{C/k_BT}-1})^2}$, yields a value for C of 2.1 cm^{-1}.

where A is the linewidth in the limit of low temperature and B is a factor that describes the rate at which the linewidth of thermally induced transitions increases with temperature. C is an activation energy of the thermally induced transitions. Using this expression, a reasonably good curve fit to the data is obtained (as shown by the solid curve in Fig. 4), yielding a value for C of 2.1 cm^{-1}, which is on the order of the width of the energy range spanned by the transitions in the B BE spectrum. This suggests that the lifetimes of individual transitions in the spectrum are likely limited by thermalization between different B BE states.

So far the discussion has been limited to spectroscopy done at zero magnetic field. In the presence of a small external magnetic field, the B BE PLE spectrum becomes much more complicated, as shown at the bottom of Fig. 5 for the ^{28}Si a sample with a field of 490 Gauss parallel to the [001] axis. In this spectrum, at least 76 transitions are resolved, and the density of these transitions is remarkable, as can be seen more clearly in the upper spectrum, which shows a magnification of the central region of the spectrum. It should be emphasized that this very rich structure reflects only transitions between the ground states of the BE and the acceptor. The application of a magnetic field results in a fourfold splitting of the neutral-acceptor ground state due to the hole degeneracy while lifting the twofold degeneracy of the electron-spin state and the fourfold degeneracies of the spin states of the two holes in the acceptor bound exciton. The splitting of the electron and hole spin states results in 18 electric-dipole-allowed transitions.[9] The valley-orbit interaction, which splits the electron states in the acceptor bound exciton into three levels at zero field, yields a fivefold splitting under an applied magnetic field along the [001] axis,[9] making for a total of 90 allowed transitions, which is only slightly higher than the number of observed transitions. Given the likelihood of accidental overlaps, it is remarkable that such a large number of the 90 possible transitions resulting from the complete removal of all degeneracies is observed.

Shallow donor and acceptor bound excitons in silicon and other indirect band-gap semiconductors have very low radia-

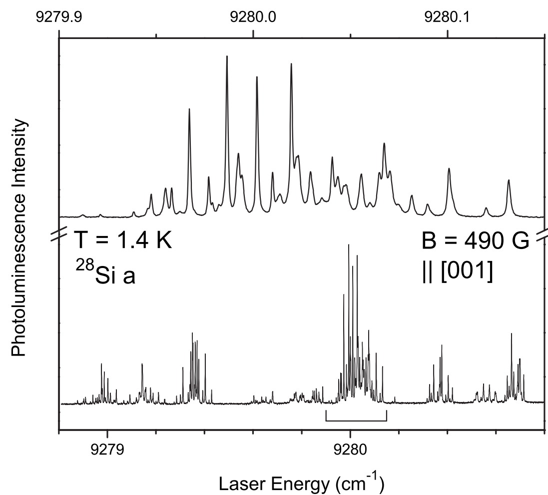

FIG. 5. The bottom spectrum shows the photoluminescence excitation signal of the boron bound exciton ground state to acceptor ground-state transitions for the ^{28}Si a sample under an applied magnetic field of 490 Gauss parallel to the [001] axis with at least 76 transitions being resolved. The region enclosed by the bracket is expanded and displayed in the upper spectrum to show the remarkable density of the transitions.

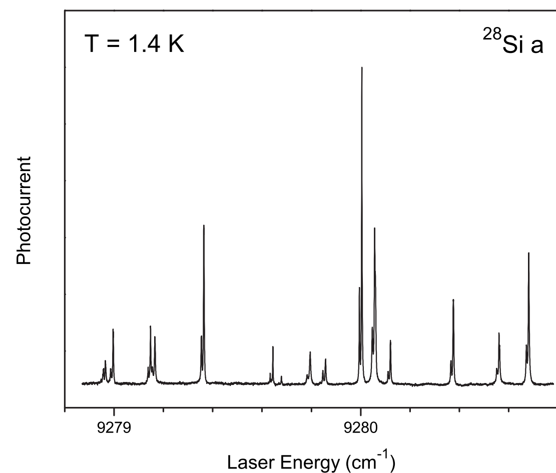

FIG. 6. Photoconductivity spectrum of the no-phonon boron bound exciton transitions for the ^{28}Si a sample. This spectrum exhibits the same fine structure that was previously seen in the PLE spectrum in Fig. 1.

tive quantum efficiencies due to the dominance of nonradiative Auger recombination.[11] The near-unity efficiency of the Auger process for these bound excitons provides an alternative approach to measuring the boron BE spectrum by detecting the free holes released in the Auger process. Simple electrical contacts were made to opposite ends of the ^{28}Si a sample by rubbing on a thin layer of In-Ga eutectic and using fine copper wires to connect an external 1.5 V bias source and a transimpedance current amplifier. Figure 6 shows a photocurrent spectrum of the boron BE that exhibits all the same features as the PLE spectrum in Fig. 1. This method of measuring BE recombination may be useful as a mechanism for the readout of the nuclear-spin state of individual ^{31}P impurities[10,18] in a silicon-based quantum-computing scheme.

IV. CONCLUSIONS

In this study we have shown the presence of 20 transitions in the no-phonon boron bound exciton spectrum in ^{28}Si using PLE spectroscopy while in earlier photoluminescence spectra only 14 components were resolved. This better resolved spectrum was also produced using photocurrent spectroscopy by detecting the free holes released in the Auger process. Each of the 20 transitions in the spectrum is a doublet with an $\sim$80/20 intensity ratio, mirroring the natural abundance ratio of ^{11}B/^{10}B. Several of the transitions exhibit a small (<0.001 cm^{-1}) inhomogeneous splitting due to the remaining isotopic randomness in the ^{28}Si samples, that scales with silicon isotopic enrichment in a similar manner to the linewidth of the unsplit transitions. In samples of higher isotopic enrichment than those available for this study, this inhomogeneous splitting is expected to vanish and even narrower linewidths are possible. Finally, we showed that by applying a small magnetic field parallel to the [001] axis, at least 76 transitions are resolved in the spectrum of the boron bound exciton ground state to acceptor ground-state transitions. This observation is yet another testament to the complex nature of the boron bound exciton, especially in comparison to the much simpler substitutional shallow donor BE spectra.[10,18]

ACKNOWLEDGMENT

This work was supported by the Natural Sciences and Engineering Research Council of Canada (NSERC).

[1] E. E. Haller, J. Appl. Phys. **77**, 2857 (1995).
[2] V. G. Plekhanov, Opt. Spectrosc. (St. Petersburg) **79**, 715 (1995).
[3] M. Cardona, Phys. Status Solidi **220**, 5 (2000) b.
[4] M. Cardona and T. Ruf, Solid State Commun. **117**, 201 (2001).
[5] M. Cardona and M. L. W. Thewalt, Rev. Mod. Phys. **77**, 1173 (2005).
[6] D. Karaiskaj, M. L. W. Thewalt, T. Ruf, M. Cardona, H.-J. Pohl, G. G. Deviatych, P. G. Sennikov, and H. Riemann, Phys. Rev. Lett. **86**, 6010 (2001).
[7] M. L. W. Thewalt and D. M. Brake, Mater. Sci. Forum **65-66**, 187 (1991).
[8] V. A. Karasyuk, A. G. Steele, A. Mainwood, E. C. Lightowlers, G. Davies, D. M. Brake, and M. L. W. Thewalt, Phys. Rev. B **45**, 11736 (1992).
[9] V. A. Karasyuk, D. M. Brake, and M. L. W. Thewalt, Phys. Rev. B **47**, 9354 (1993).
[10] M. L. W. Thewalt, A. Yang, M. Steger, D. Karaiskaj, M. Cardona, H. Riemann, N. V. Abrosimov, A. V. Gusev, A. D. Bulanov, I. D. Kovalev, A. K. Kaliteevskii, O. N. Godisov, P.

Becker, H. J. Pohl, E. E. Haller, J. W. Ager III, and K. M. Itoh, J. Appl. Phys. **101**, 081724 (2007).

[11] W. Schmid, Phys. Status Solidi **84**, 529 (1977) b.

[12] V. Heine and C. H. Henry, Phys. Rev. B **11**, 3795 (1975).

[13] J. R. Haynes, Phys. Rev. Lett. **4**, 361 (1960).

[14] M. Steger, A. Yang, D. Karaiskaj, M. L. W. Thewalt, E. E. Haller, J. W. Ager III, M. Cardona, H. Riemann, N. V. Abrosimov, A. V. Gusev, A. D. Bulanov, A. K. Kaliteevskii, O. N. Godisov, P. Becker, and H.-J. Pohl, Phys. Rev. B **79**, 205210 (2009).

[15] M. Steger, A. Yang, D. Karaiskaj, M. L. W. Thewalt, E. E. Haller, J. W. Ager III, M. Cardona, H. Riemann, N. V. Abrosimov, A. V. Gusev, A. D. Bulanov, A. K. Kaliteevskii, O. N. Godisov, P. Becker, H.-J. Pohl, and K. M. Itoh, in *Physics of Semiconductors: 28th International Conference on the Physics of Semiconductors—ICPS 2006*, AIP Conf. Proc. No. 893 (AIP, New York, 2007), p. 231.

[16] D. Karaiskaj, J. A. H. Stotz, T. Meyer, M. L. W. Thewalt, and M. Cardona, Phys. Rev. Lett. **90**, 186402 (2003).

[17] D. Karaiskaj, M. L. W. Thewalt, T. Ruf, M. Cardona, and M. Konuma, Phys. Rev. Lett. **89**, 016401 (2002).

[18] A. Yang, M. Steger, D. Karaiskaj, M. L. W. Thewalt, M. Cardona, K. M. Itoh, H. Riemann, N. V. Abrosimov, M. F. Churbanov, A. V. Gusev, A. D. Bulanov, A. K. Kaliteevskii, O. N. Godisov, P. Becker, H.-J. Pohl, J. W. Ager III, and E. E. Haller, Phys. Rev. Lett. **97**, 227401 (2006).